Journal of Electron Spectroscopy and Related Phenomena 172 (2009) 42–46

Contents lists available at ScienceDirect

Journal of Electron Spectroscopy and Related Phenomena

journal homepage: www.elsevier.com/locate/elspec

Oriented self-assembled monolayers of bifunctional molecules on InAs

R. Stine [a], D.Y. Petrovykh [a,b,*]

[a] Naval Research Laboratory, Washington, DC 20375, USA
[b] Department of Physics, University of Maryland, College Park, MD 20742, USA

ARTICLE INFO

Article history:
Available online 13 February 2009

Keywords:
X-ray photoelectron spectroscopy
Indium arsenide
Thiol
Self-assembled monolayers
Bifunctional
Oriented
Functionalization

ABSTRACT

We describe the formation and characterization of oriented self-assembled monolayers (SAMs) of bifunctional molecules on InAs. Cysteamine, a small molecule with thiol and amine termini, can be efficiently deposited on InAs(001) from a basic aqueous solution. Analysis of the deposited films using X-ray photoelectron spectroscopy (XPS) reveals that cysteamine forms a monolayer, in which molecules are oriented and attached to the InAs surface exclusively via their thiol termini. The free amine ligands presented at the interface of the resulting oriented SAM should provide a convenient pathway for subsequent surface functionalization. In addition, cysteamine deposition efficiently removes InAs native oxides; the resulting cysteamine SAM provides surface passivation, protecting the InAs substrate from reoxidation after short-term exposures to air and aqueous solutions.

1. Introduction

Deposition of self-assembled monolayers (SAMs) [1,2] is a promising approach for surface passivation and functionalization of III–V semiconductors [3–12]. Much of the recent progress focused on chemical and electronic surface passivation provided by thiol-based SAMs, which have been observed to inhibit surface oxidation [13–17] and to enhance photoluminescence [18–20] of III–V materials. Many passivation effects of SAMs are similar to those observed for III–V surfaces treated by inorganic and organic sulfides [4,21–30]. In contrast to the numerous demonstrations of III–V surface passivation, relatively few studies have reported successful functionalization of III–V surfaces by SAMs, e.g., via the deposition of bifunctional SAMs [10–13]. Creating SAMs that present reactive ligands at the interface is critical for functional applications, including the construction of multilayers or attachment of biological molecules.

Producing oriented bifunctional monolayers on InAs and other III–V materials, however, has proven to be challenging. Whereas on coinage metals the thiol-down orientation of SAMs is largely independent of their terminal functionality [1,2], the same rule does not hold for thiols on III–V surfaces. Our examination of XPS spectra from previous studies [11,13] indicates, for example, that III–V surfaces exposed to alkanethiols with oxygen-containing functional groups (hydroxyls and carboxyls) show considerable oxidation, presumably because oxygen-containing ligands readily interact with III–V semiconductors. The resulting oxygen-based attachment chemistry not only leads to disordered monolayers, but also produces surface oxidation that can have detrimental effects on electronic properties of the interface [3,4,14,21,22].

Surprisingly, the use of thiol molecules functionalized with amines rather than oxygen-based ligands has been largely left unexamined on InAs or other III–V materials. Here, we present a comprehensive XPS analysis of cysteamine monolayers formed on InAs, and show that oriented films can be produced presenting amine ligands suitable for further chemical or biological functionalization. These monolayers also offer surface passivation, protecting the InAs substrate from reoxidation after short-term exposures to air and aqueous solutions.

2. Experimental

InAs (0 0 1) samples were diced from a commercial single side polished wafer. Cysteamine ($HSC_2H_4NH_2$, 98% purity) was purchased from Sigma–Aldrich (St. Louis, MO). Prior to treatment, InAs samples were degreased by soaking in hexanes for 24 h, then sonicated sequentially in hexanes, acetone, and ethanol, for 5 min in each solvent. Samples were then rinsed with ethanol and dried under flowing nitrogen.

Cysteamine solution consisted of 10 mM cysteamine in a 1:9 mixture of NH_4OH (29.7% stock solution, Fisher Scientific) in absolute ethanol. The alkaline component of the solution strips the native oxide from the InAs sample and simultaneously de-protonates the thiol group, thus activating it for covalent attachment to the surface [7,14,17]. Monolayers were deposited by immersing InAs samples in the cysteamine solution for 30 min, in glass scintillation vials placed in a water bath at 55 °C. After treat-

* Corresponding author at: Code 6176, Naval Research Laboratory, 4555 Overlook Ave. SW, Washington, DC 20375, USA. Tel.: +1 202 404 3381; fax: +1 202 767 3321.
E-mail address: dmitri.petrovykh@nrl.navy.mil (D.Y. Petrovykh).

0368-2048/$ – see front matter © 2009 Elsevier B.V. All rights reserved.
doi:10.1016/j.elspec.2009.02.001

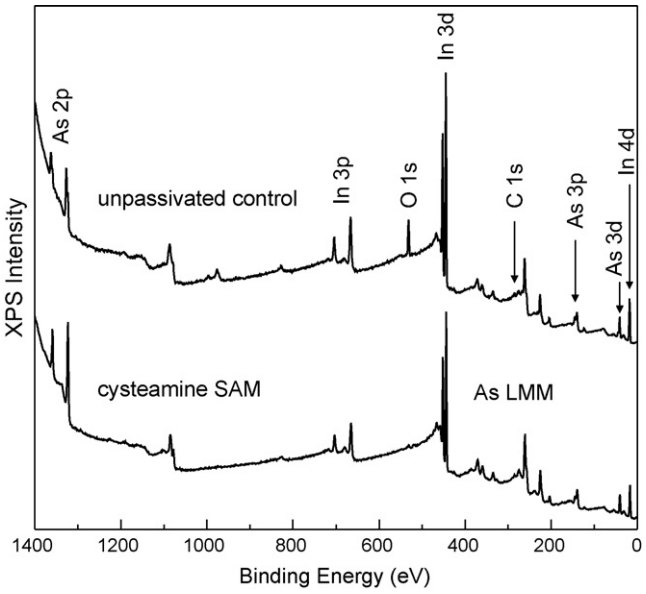

Fig. 1. Survey spectra of InAs samples treated in basic solutions with and without cysteamine. The basic solution without cysteamine was used to remove native oxides from the unpassivated control (top spectrum), the cysteamine SAM (bottom spectrum) was deposited from a similar basic solution containing cysteamine. Exposure to air for ≤10 min before XPS analysis reoxidized only the unpassivated control (O 1s peak in top spectrum).

ment, samples were rinsed in copious amounts of deionized water and dried with flowing nitrogen.

The basic solution used for cysteamine deposition removes native oxide from InAs substrates, therefore samples stripped of their native oxide using a similar treatment (but without cysteamine in solution) are most appropriate as controls for determining the chemical effects of the cysteamine deposition and for separating them from the effects of the basic solution. The use of dilute NH_4OH to produce high-quality oxide-free GaAs substrates for deposition of SAMs [7,14] suggested a similar method for InAs. The InAs control samples (also denoted as "unpassivated" controls hereafter) were stripped of native oxide by placing them for 10 min into a solution of 15% NH_4OH in deionized water. Samples were then rinsed with deionized water and dried under flowing nitrogen, immediately prior to transferring them into the vacuum chamber for XPS analysis.

XPS characterization was performed in a commercial XPS system equipped with a monochromatic Al Kα source, a magnetic lens, and a hemispherical electron energy analyzer (58° angle between the monochromator and analyzer) [30–32]. XPS measurements were carried out without any additional sample treatment, at room temperature in a UHV chamber with base pressure $<1 \times 10^{-9}$ Torr. Nominal X-ray spot size and analyzer field of view were $\leq 1\,mm^2$, the nominal acceptance angles were 4° and 30° (along the energy dispersive and nondispersive directions, respectively), no effort was made to ensure a particular azimuthal alignment of samples. The binding energies (BE) are reported with 0.1 eV precision, based on a two-point analyzer energy calibration described in detail elsewhere [30–32]. The elemental XPS data (nominal analyzer resolution of 0.36 eV) were acquired in angle-integrated normal emission mode and analyzed following previously described procedures [28–32].

3. Results and discussion

3.1. XPS surveys

The XPS surveys in Fig. 1 compare the surface compositions of two InAs samples that were treated in similar basic solutions and briefly exposed to deionized water and ambient air before XPS measurements. The O 1s intensity is clearly dramatically higher for the "unpassivated" control sample (top spectrum in Fig. 1), the surface of which was etched in a basic solution but left apparently unprotected against subsequent reoxidation. In contrast, the spectrum of the sample treated by a cysteamine-containing basic solution (bottom spectrum in Fig. 1) exhibits a much weaker O 1s peak, indicating that the cysteamine deposition not only removed the native oxide but also provided short-term passivation against reoxidation.

In addition to direct surface oxidation, water adsorption can also contribute to the O 1s signal, particularly because cysteamine deposition is expected to produce a hydrophilic surface [33]. The low O 1s signal intensity makes any detailed peak fitting in that region ambiguous, but the overall width of 3–4 eV for the O 1s spectral envelope indicates that multiple chemical states of oxygen are present on the surface. A definitive assignment of some O 1s intensity as adsorbed water is prevented by the lack of reliable reference data on O 1s BEs for this system. The total O 1s signal, however, is comparable, within the experimental uncertainties, to the total signal from the surface oxides, which suggests ≈1 monolayer (ML) as the upper limit on the total amount of adsorbed water molecules, based on our previous coverage estimates for passivated InAs surfaces [30]. The low limit on the amount of surface-bound water in UHV, of course, does not rule out the presence of water on these surfaces under ambient conditions, but rather indicates that physisorbed water molecules are effectively removed from cysteamine-treated surfaces under UHV conditions.

Overall, both surveys in Fig. 1 are dominated by major peaks of the substrate elements, In and As. In fact, As-based III–V materials provide particularly convenient internal references for semi-quantitative evaluation of spectroscopic signatures of small-thiol adsorbates, because the substrate As LMM Auger and As 3p XPS peaks are adjacent to the C 1s and S 2p regions, respectively. In general, even a complete monolayer of small thiol-containing molecules will produce C 1s and S 2p peaks that are much weaker than the substrate peaks, so the low intensity of cysteamine spectroscopic signatures in the bottom survey in Fig. 1 is expected, rather than surprising. The barely noticeable C 1s peaks in Fig. 1 also indicate that nonspecific adsorption of organic contaminants was not significant for either of the two samples.

In order to directly examine the spectroscopic signatures of cysteamine and the associated InAs interface chemistry, in the following sections we consider the high-resolution elemental spectra (Fig. 2) and peak fitting results (Tables 1 and 2) for the two samples introduced in Fig. 1. The spectra in Fig. 2 are normalized to the bulk As 3d component *for each sample*, to enable direct semi-quantitative

Table 1
Fitting parameters of major XPS peaks for a cysteamine monolayer on InAs.

Peak	Component	BE (eV)	FWHM (eV)	
			Lorentzian	Gaussian
As $2p_{3/2}$	As–In	1322.8	0.5	1.0
	As–S	1324.0	0.5	1.5
	As^{3+} oxide	1326.2	0.5	1.5
	As^{5+} oxide	1327.3	0.5	1.5
In $3d_{5/2}$	In–As	444.5	0.3	0.5
	In–S	445.0	0.3	0.5
	In–O	445.3	0.3	1.2
N 1s	N–C	400.0	0.2	1.3
S $2p_{3/2}$	Thiolate	162.5	0.1	1.1
	Chemisorbed sulfur	161.0	0.1	1.1
As $3d_{5/2}$	As–In	40.9	0.1	0.6
	As–S	41.9	0.1	0.6
	As–O	44.2	0.1	1.2

Table 2
Normalized intensities of XPS peaks for a cysteamine monolayer on InAs and for etched unpassivated InAs.

Peak	Component	Normalized intensity	
		Cysteamine on InAs	Unpassivated InAs control
As $2p_{3/2}$	As–In	0.941	0.56
	As–S	0.25	–
	As^{3+} oxide	0.08	0.76
	As^{5+} oxide	–	0.31
O 1s	Total signal	0.1	2.2
In $3d_{5/2}$	In–As	1.2	1.5
	In–S	0.09	–
	In–O	–	1.0
N 1s	Total signal	0.11	–
C 1s	Total signal	0.39	0.43
S $2p_{3/2}$	Thiolate	0.091	–
	Chemisorbed sulfur	0.027	–
As $3d_{5/2}$	As–In	1.0	1.0
	As–S	0.033	–
	As–O	–	0.19

The normalization factor for each peak includes Scofield photoelectric cross-section [45], analyzer transmission function, and electron attenuation length (EAL) [30]. For each sample, the peaks have been normalized to the bulk component of As 3d (see Fig. 2).

comparison between the samples. For each elemental region, the *y*-axis scale is adjusted *for both samples* by an arbitrary coefficient to compensate for the dramatically different elemental peak intensities. For quantitative comparison, in Table 2 the peak intensities from Fig. 2 are listed with additional normalization that includes element-specific and instrument factors.

3.2. Interface chemistry signatures in S 2p region

For thiol-based SAMs and sulfur passivated III–V surfaces, the S 2p peaks provide the direct means for evaluating sulfur attachment chemistry and for quantifying surface coverage [7,9,14–16,30,31,33–37]. The fit in the S 2p region shows two sulfur species present at the surface, one at BE of 162.5 eV (shaded in Fig. 2e), and a smaller secondary peak at 161 eV (thin line in Fig. 2e). The absence of spectral features with BE ≥163.5 eV in S 2p region indicates that there are no free thiol groups in these films [31,34,37].

The BE of the main S 2p doublet in Fig. 2e is consistent with that of thiolates on III–V semiconductors [7,9,14–16,34]. The low-BE minority component most likely corresponds to sulfur chemisorbed on the InAs surface, but the origin of such a sulfur species is ambiguous because there are at least two plausible sources suggested by the literature [34–39]. Most commonly, the S 2p components with BE below the main thiolate doublet are assigned as sulfur that has been cleaved from the organic component; surface reactions involving such C–S bond scission have been reported on metals [38,39] and on GaAs [34]. The second possibility is the adsorption of sulfur that was present as a contaminant in the reaction solution [37].

For samples in this study, the observed ratio of sulfur to nitrogen is 1.1 (Table 2), i.e., higher than expected from stoichiometry of cysteamine. The presence of the excess sulfur is consistent with either mechanism described above, because both result in adsorbed sulfur that is not part of a cysteamine molecule and our experimental conditions (basic solution at elevated temperature) could potentially favor one or both processes. Indirect evidence of a possible common contaminant in commercial cysteamine samples is provided by the previous observations of a similar low-BE S 2p component in cysteamine monolayers on gold [33,36], which do not share substrate or deposition conditions with our work.

The intensity ratios between S 2p and the substrate peaks provide a quantitative estimate of the surface coverage. A previous study from our laboratory on quantification of sulfur and oxide monolayers for sulfur-passivated InAs surfaces suggests that two intensity ratios can be particularly useful for estimating the sulfur coverage [30]. First is the ratio of S 2p intensity to that of the main (bulk As–In) component of the As 3d peak (S 2p/$As_{As–In}$ 3d), which is very stable empirically because the bulk As 3d can be identified and fit unambiguously for these types of surfaces [30]. The second useful intensity ratio is between the S 2p peak and the total intensity of the In $3d_{5/2}$ peak (S 2p/In $3d_{5/2}$), which can be rigorously quantified for sulfur on InAs [30].

The intensity ratios measured for the cysteamine films in this work are S 2p/$As_{As–In}$ 3d = 0.12 and S 2p/In $3d_{5/2}$ = 0.013; the corresponding estimate of the sulfur coverage is 0.8 ± 0.1 ML, where 1 ML = 5.41×10^{14} cm^{-2} is the atomic surface density of InAs(001) [30]. Combined with the absence of S 2p signal from free thiols,

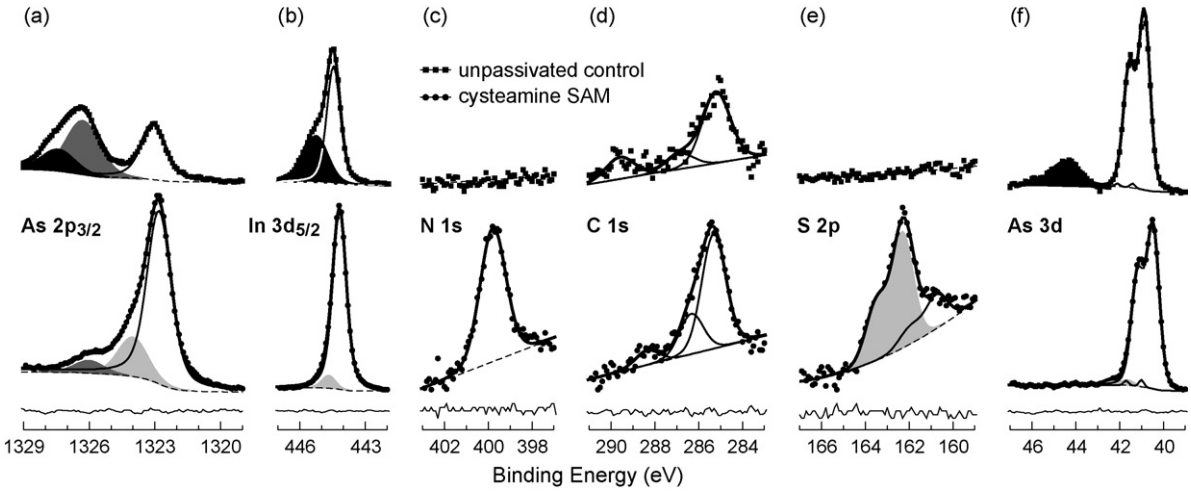

Fig. 2. High-resolution elemental signatures of cysteamine deposition on InAs. The cysteamine SAM (circles) and the unpassivated control (squares) were prepared in similar basic solutions with and without cysteamine, respectively. The specific N 1s and S 2p peaks and thiolate signatures [gray shading in (a), (b), (e), and (f)] are observed only after cysteamine deposition. After ≤10 min in air, significant oxidation signatures [dark gray and black shading in (a), (b), and (f)] are only observed for the unpassivated control (top spectra). Symbols = data points; thick black lines = overall fits; thin lines and shading = component fits; dashed lines = backgrounds; a representative fit residual is shown at the bottom of each panel. For each sample (horizontal row) intensities are normalized to the bulk As 3d component, in order to provide semi-quantitative comparison *between the two samples*, i.e., for each pair of elemental regions. Due to significant disparities between the elemental peak intensities (see Fig. 1), the relative elemental intensities within each row are *not* quantitative, see Table 2 for the corresponding normalized peak intensities.

the coverage estimate confirms that cysteamine was deposited as a monolayer under the conditions used in this work.

3.3. Amine chemistry signatures in N 1s region

The N 1s peak appears at BE = 400 eV (Fig. 2c and Table 1), which is consistent with BE previously reported for free amine groups in close proximity to sulfur [40–42] and for cysteamine on gold [33,36]. In addition, no significant intensity appears in the 396–398 eV BE range that typically corresponds to nitrogen atoms chemisorbed on an inorganic substrate, e.g., as reported for amines in DNA bases chemisorbed on Au [32] and on oxidized GaAs [43]. In other words, there is no evidence of amine ligands involved in the surface attachment of cysteamine monolayers. The N 1s peak thus can be unambiguously assigned as the signature of free amine ligands presented at the top interface of the cysteamine monolayer.

3.4. Stoichiometry and C 1s spectra

Unlike the S 2p and N 1s peaks that only appear in spectra after the cysteamine deposition, the peaks in C 1s region are of comparable intensity for the cysteamine sample and for the control that was simply etched in a basic solution (Fig. 2 and Table 2). In both cases the C 1s intensity is much smaller than that of the adjacent As LMM Auger substrate peak (Fig. 1), indicating that carbonaceous contaminants did not overwhelm either surface. The presence of carbon contamination on the unpassivated control sample, however, indicates that similar contamination may be present on the cysteamine sample as well.

The presence of C 1s components with BEs around 286 and 288 eV for the cysteamine sample (Fig. 2d) is consistent with C 1s spectra previously reported for cysteamine on gold [33], so the cysteamine contribution likely dominates the C 1s spectrum in this case. For a more quantitative evaluation, we consider the carbon-to-nitrogen elemental ratio, which is approximately 4:1 for the cysteamine sample (Table 2), thus indicating that about half of the carbon on the surface can be from contamination, including that from solution and adventitious sources. This relatively small amount of carbon contamination is somewhat surprising for a sample that presents a reactive free amine interface during treatments in organic solvents and exposure to ambient air.

3.5. InAs substrate peaks and surface passivation

A detailed examination of the In and As substrate peaks in Fig. 2a, 2b, and 2f reveals trends in the InAs interface chemistry that are consistent with a surface passivation effect of the cysteamine monolayer. In Section 3.1 we have already observed that surface reoxidation of the unpassivated control sample was dramatically higher than that of the cysteamine-treated sample (compare the intensity of O 1s peaks in Fig. 1 and Table 2).

Large oxide components (Table 1, black shading in Fig. 2b and 2f) appear in the In 3d and As 3d spectra for the unpassivated control sample. The original native oxide on this sample was stripped in NH_4OH before the spectra were acquired, so the surface oxide seen for the control sample in Fig. 2 grew in the approximately 10 min of air exposure while transferring into the XPS system. In contrast, after cysteamine deposition the oxide peaks are not present in the In 3d and As 3d regions (bottom spectra in Fig. 2b and 2f), despite an atmospheric exposure similar to that of the control sample. Instead, sulfide components with chemical shifts smaller than those of the oxides (Table 1) can be observed in both In 3d and As 3d spectra (light gray shading in Fig. 2b and 2f).

The passivation effect of the cysteamine monolayer is even more pronounced in the surface sensitive [30] As $2p_{3/2}$ spectra in Fig. 2a. The large As^{3+} (dark gray shading) and As^{5+} (black shading) oxide peaks at 1326.2 eV and 1327.3 eV, respectively, are observed for the unpassivated control sample, but are largely absent following the cysteamine deposition, and a distinct As–S component appears at 1324 eV (light gray shading). The presence of As–S on this surface is interesting, because other sulfur passivation techniques in basic solutions have not shown any appreciable As–S bond formation on InAs, with sulfide formation limited almost exclusively to In–S [28–30]. The observed difference in interface composition between conventional sulfur passivation and small thiol attachment on InAs could be due to a more difficult removal of As–S species produced by the monovalent chemisorption of the thiolate sulfur.

4. Cysteamine monolayers on InAs

All the individual results of the detailed XPS analysis and interpretation presented in Section 3 are consistent with us having successfully deposited approximately one monolayer of cysteamine on InAs. The constituent cysteamine molecules in this monolayer are covalently bound to both In and As atoms of the substrate and present free amine ligands at the top interface of the monolayer. In addition to directly observing spectral signatures of oriented cysteamine molecules, we see no evidence of multilayer formation, free thiol ligands, or substrate-bound amine ligands in these cysteamine monolayers. While the possibility of pinhole defects in these SAMs cannot be excluded based on XPS data acquired from $\approx$1 mm^2 areas, the quantitative analysis of the S/As and S/In ratios (Section 3.2) and the prevention of rapid surface reoxidation both indicate a nearly complete monolayer coverage.

In our procedure, the reaction time used for the deposition of these monolayers was much shorter than the soaking time used to deposit and equilibrate the benchmark SAMs of alkanethiols on GaAs surfaces [7,14], so despite the higher temperature that we used, the formation of these cysteamine monolayers was likely a kinetically controlled rather than a quasi-equilibrium process. The faster deposition, however, allowed us to produce oxide-free interfaces while avoiding the complications of de-oxygenating the reaction solutions—an important practical consideration for creating functionalized surfaces [12]. The complex interplay of reaction rates (surface etching, thiol adsorption, and oxidation) and solution parameters involved in our method may also explain why we have not been able to generalize this approach for depositing SAMs of oriented amino-thiols with longer carbon chains, even though such an extension may seem to be straightforward.

Our ability to obtain critical structural information about monolayers of small bifunctional molecules validates the choice of XPS as a quantitative analytical technique for such characterization [44]. Cysteamine monolayers, in fact, are a good example of a system for which XPS is one of the few traditional characterization techniques that can provide reliable quantitative results. For such short molecules, the nominal thickness of the resulting monolayers falls into the sub-nm range, i.e., below the limits of applicability of ellipsometry and atomic force microscopy (AFM). Combined with a poorly reflecting semiconductor substrate such as InAs, the small size of the deposited molecules would also require a heroic effort to perform meaningful infrared spectroscopy for such monolayers. As passivation and functionalization of surfaces for practical applications [2,4] often is achieved using organic monolayers that share the challenging properties of these cysteamine SAMs, we believe that our demonstration of a comprehensive and quantitative XPS analysis will provide a baseline and guidance for similar future analyses.

5. Conclusions

We have demonstrated that oriented SAMs can be produced on InAs surfaces by deposition of bifunctional cysteamine molecules

from ethanolic solutions under basic conditions. The reactive amine functionality presented at the top interface of these monolayers opens interesting possibilities for future applications of functionalized InAs surfaces in biosensors or multilayer film growth [4,7,28]. Furthermore, the cysteamine SAM appears to provide surface passivation for the InAs surface, protecting against reoxidation during short-term exposures to aqueous environment and ambient air. In most practical applications that we foresee for small bifunctional molecules, reactive amine ligands are either encapsulated/capped against long-term exposure or added as a small fraction of a mixed passivating monolayer. The observed short-term stability of our model monolayers then suggests that a similar method can be used to incorporate oriented bifunctional molecules into more complex passivated and functionalized surfaces.

Acknowledgments

R.S. acknowledges the support of an ASEE Postdoctoral Research Associateship. This work was funded by the Defense Threat Reduction Agency (DTRA) Joint Science and Technology Office for Chemical and Biological Defense, the Office of Naval Research (ONR), and the Air Force Office of Scientific Research (AFOSR).

References

[1] D.K. Schwartz, Annu. Rev. Phys. Chem. 52 (2001) 107.
[2] J.C. Love, L.A. Estroff, J.K. Kriebel, R.G. Nuzzo, G.M. Whitesides, Chem. Rev. 105 (2005) 1103.
[3] O. Voznyy, J.J. Dubowski, J. Phys. Chem. C 112 (2008) 3726.
[4] F. Seker, K. Meeker, T.F. Kuech, A.B. Ellis, Chem. Rev. 100 (2000) 2505.
[5] C.W. Sheen, J.X. Shi, J. Martensson, A.N. Parikh, D.L. Allara, J. Am. Chem. Soc. 114 (1992) 1514.
[6] O.S. Nagagawa, S. Ashok, C.W. Sheen, J. Martensson, D.L. Allara, Jpn. J. Appl. Phys. 30 (1991) 3759.
[7] C.L. McGuiness, A. Shaporenko, C.K. Mars, U. Sundararajan, M. Zharnikov, D.L. Allara, J. Am. Chem. Soc. 128 (2006) 5231.
[8] T.A. Tanzer, P.W. Bohn, I.V. Roshchin, L.H. Greene, J.F. Klem, Appl. Phys. Lett. 75 (1999) 2794.
[9] A. Shaporenko, K. Adlkofer, L.S.O. Johansson, M. Tanaka, M. Zharnikov, Langmuir 19 (2003) 4992.
[10] A. Shaporenko, K. Adlkofer, L.S.O. Johansson, A. Ulman, M. Grunze, M. Tanaka, M. Zharnikov, J. Phys. Chem. B 108 (2004) 17964.
[11] H. Ohno, L.A. Nagahara, W. Mizutani, J. Takagi, H. Tokumoto, Jpn. J. Appl. Phys. 38 (1999) 180.
[12] Y. Jun, X.Y. Zhu, J.W.P. Hsu, Langmuir 22 (2006) 3627.
[13] D.M. Wieliczka, X. Ding, J.J. Dubowski, J. Vac. Sci. Technol. A 24 (2006) 1756.
[14] C.L. McGuiness, A. Shaporenko, M. Zharnikov, A.V. Walker, D.L. Allara, J. Phys. Chem. C 111 (2007) 4226.
[15] H. Lim, C. Carraro, R. Maboudian, M.W. Pruessner, R. Ghodssi, Langmuir 20 (2004) 743.
[16] O. Dassa, V. Sidorov, Y. Paz, D. Ritter, J. Electrochem. Soc. 153 (2006) G91.
[17] T. Baum, S. Ye, K. Uosaki, Langmuir 15 (1999) 8577.
[18] S.R. Lunt, G.N. Ryba, P.G. Santangelo, N.S. Lewis, J. Appl. Phys. 70 (1991) 7449.
[19] K. Moumanis, X. Ding, J.J. Dubowski, E.H. Frost, J. Appl. Phys. 100 (2006) 034702.
[20] X. Ding, K. Moumanis, J.J. Dubowski, L. Tay, N.L. Rowell, J. Appl. Phys. 99 (2006) 054701.
[21] C.J. Sandroff, R.N. Nottenburg, J.C. Bischoff, R. Bhat, Appl. Phys. Lett. 51 (1987) 33.
[22] M.S. Carpenter, M.R. Melloch, M.S. Lundstrom, S.P. Tobin, Appl. Phys. Lett. 52 (1988) 2157.
[23] J.F. Fan, H. Oigawa, Y. Nannichi, Jpn. J. Appl. Phys. 27 (1988) L1331.
[24] Y. Fukuda, Y. Suzuki, N. Sanada, M. Shimomura, S. Masuda, Phys. Rev. B 56 (1997) 1084.
[25] M.J. Lowe, T.D. Veal, C.F. McConville, G.R. Bell, S. Tsukamoto, N. Koguchi, Surf. Sci. 523 (2003) 179.
[26] E.D. Lu, F.P. Zhang, S.H. Xu, X.J. Yu, P.S. Xu, Z.F. Han, F.Q. Xu, X.Y. Zhang, Appl. Phys. Lett. 69 (1996) 2282.
[27] F.Q. Xu, E.D. Lu, H.B. Pan, C.K. Xie, P.S. Xu, X.Y. Zhang, Surf. Rev. Lett. 8 (2001) 19.
[28] D.Y. Petrovykh, M.J. Yang, L.J. Whitman, Surf. Sci. 523 (2003) 231.
[29] D.Y. Petrovykh, J.P. Long, L.J. Whitman, Appl. Phys. Lett. 86 (2005) 242105.
[30] D.Y. Petrovykh, J.M. Sullivan, L.J. Whitman, Surf. Interf. Anal. 37 (2005) 989.
[31] D.Y. Petrovykh, H. Kimura-Suda, A. Opdahl, L.J. Richter, M.J. Tarlov, L.J. Whitman, Langmuir 22 (2006) 2578.
[32] D.Y. Petrovykh, H. Kimura-Suda, M.J. Tarlov, L.J. Whitman, Langmuir 20 (2004) 429.
[33] M. Wirde, U. Gelius, L. Nyholm, Langmuir 15 (1999) 6370.
[34] S. Donev, N. Brack, N.J. Paris, P.J. Pigram, N.K. Singh, B.F. Usher, Langmuir 21 (2005) 1866.
[35] O. Cavalleri, G. Gonella, S. Terreni, M. Vignolo, P. Pelori, L. Floreano, A. Morgante, M. Canepa, R. Rolandi, J. Phys.: Condens. Matter 16 (2004) S2477.
[36] S.Y. Lee, J. Noh, E. Ito, H. Lee, M. Hara, Jpn. J. Appl. Phys. 42 (2003) 236.
[37] C.J. Zhong, R.C. Brush, J. Anderegg, M.D. Porter, Langmuir 15 (1999) 518.
[38] G. Gonella, O. Cavalleri, S. Terreni, D. Cvetko, L. Floreano, A. Morgante, M. Canepa, R. Rolandi, Surf. Sci. 566 (2004) 638.
[39] Y.H. Lai, C.T. Yeh, S.H. Cheng, P. Liao, W.H. Hung, J. Phys. Chem. B 106 (2002) 5438.
[40] R. Srinivasan, R.A. Walton, Inorg. Chim. Acta 25 (1977) L85.
[41] T.H. Lee, J.W. Rabalais, J. Electron. Spectrosc. Relat. Phenom. 11 (1977) 123.
[42] V.I. Nefedov, I.B. Baranovskii, A.K. Molodkin, V.O. Omuralieva, Zh. Neorg. Khim. 18 (1973) 1295.
[43] L. Mohaddes-Ardabili, L.J. Martinez-Miranda, J. Silverman, A. Christou, L.G. Salamanca-Riba, M. Al-Sheikhly, Appl. Phys. Lett. 83 (2003) 192.
[44] A.S. Duwez, J. Electron Spectrosc. Relat. Phenom. 134 (2004) 97.
[45] J.H. Scofield, J. Electron Spectrosc. Relat. Phenom. 8 (1976) 129.